Bystin in human cancer cells: intracellular localization and function in ribosome biogenesis

Masaya MIYOSHI*, Tetsuya OKAJIMA*, Tsukasa MATSUDA*, Michiko N. FUKUDA†, and Daita NADANO*[1]

*Department of Applied Molecular Biosciences, Graduate School of Bioagricultural Sciences, Nagoya University, Nagoya 464-8601, Japan, and †Burnham Institute for Medical Research, North Torrey Pines Rd, La Jolla, CA 92037, USA

Short title: Bystin in HeLa cells

Abbreviations used: ActD, actinomycin D; mTOR, mammalian target of rapamycin; RNAi, RNA interference; RT, reverse transcription; siRNA, small interfering RNA.

[1] To whom correspondence should be addressed:

Daita Nadano, Ph. D.

Associate Professor

Department of Applied Molecular Biosciences

Graduate School of Bioagricultural Sciences

Nagoya University

Furo-cho, Chikusa, Nagoya 464-8601, Japan

Phone: +81-52-789-4130

Fax: +81-52-789-4128

E-mail: nadano@agr.nagoya-u.ac.jp

Synopsis

While bystin has been identified as a protein potentially involved in human embryo implantation—a process unique to mammals—the bystin gene is evolutionarily conserved from yeast to humans. DNA microarray data indicates that bystin is overexpressed in human cancers, suggesting that it promotes cell growth. We undertook RT-PCR and immunoblotting and confirmed that bystin mRNA and protein, respectively, is expressed in human cancer cell lines, including HeLa. Subcellular fractionation identified bystin protein as nuclear and cytoplasmic, and immunofluorescence showed that nuclear bystin localizes mainly in the nucleolus. Sucrose gradient ultracentrifugation of total cytoplasmic ribosomes revealed preferential association of bystin with the 40S subunit fractions. To analyze its function, bystin expression in cells was suppressed by RNA interference. Pulse-chase analysis of ribosomal RNA processing suggested that bystin knockdown delays processing of 18S ribosomal RNA, a component of the 40S subunit. Furthermore, this knockdown significantly inhibited cell proliferation. Our findings suggest that bystin may promote cell proliferation by facilitating ribosome biogenesis, specifically in the production of the 40S subunit. Localization of bystin to the nucleolus, the site of ribosome biogenesis, was blocked by low concentrations of actinomycin D, a reagent causing nucleolar stress. When bystin was transiently overexpressed in HeLa cells subjected to nucleolar stress, nuclear bystin was included in particles different from the nuclear stress granules induced by heat shock. By contrast, cytoplasmic bystin was barely affected by nucleolar stress. These results suggest that, while bystin may play multiple roles in mammalian cells, a conserved function is to facilitate ribosome biogenesis required for cell growth.

Keywords: *BYSL*, cancer, embryo implantation, nucleolar stress, ribosomal RNA processing, ribosome biogenesis.

INTRODUCTION

Embryo implantation is an essential step in the early phase of mammalian development [1]. In humans, a fertilized egg grows into the blastocyst, attaches to the endometrial epithelium of the uterus, and aggressively invades maternal uterine tissue, a process required for development of the placenta [2]. Histological studies indicate similarities between embryo implantation and metastasis and invasion of malignant tumors [3]. For example, a family of cell adhesion molecules, integrins, functions in the angiogenesis of implantation and metastasis [4]. Therefore, analysis of implantation mechanisms can shed light into cancer progression.

An intrinsic membrane protein, trophinin, mediates homophilic cell adhesion [5]. Because it is expressed on the apical surfaces of the trophectoderm of the blastocyst and endometrium at the period of implantation, adhesion mediated by trophinin is considered the first step in embryo implantation followed by invasion of human embryos [5]. In addition to its implantation role, trophinin is upregulated in testicular germ cell tumors and likely functions in tumor metastasis [6]. Trophinin forms a functional complex with two cytoplasmic proteins, tastin and bystin [5, 7, 8]. Both render trophinin an active cell adhesion molecule. Tastin and bystin exhibit no known functional domain or motif, and their properties and regulation are still largely uncharacterized.

Embryo implantation is unique to mammals. Our genetic database search shows no genes encoding homologues of the trophinin (*TRO*) and tastin (*TROAP*) genes in organisms other than mammals. By contrast, the human bystin gene (*BYSL*) has homologues in other eukaryotes. Homologues of the bystin gene are also found in *Drosophila* and budding yeast (*Saccharomyces cerevisiae*) and designated bys [9] and ENP1 [10], respectively. Because the amino acid sequence homology of the human, *Drosophila*, and yeast protein products is very high [11], fly Bys and yeast Enp1

proteins are considered orthologues of mammalian bystin.

Drosophila Bys shows a dynamic expression pattern compatible with a role in cell-cell interaction and proliferation [9]. Both human bystin and fly Bys are targets of the growth-regulating transcription factor, Myc [9, 12]. Enp1 has been identified as an essential nuclear protein in yeast [10]. A temperature-sensitive ENP1-null mutant showed defective processing of ribosomal RNA (rRNA), although expression of human bystin did not complement the yeast null mutant [11]. The mouse bystin gene (*Bysl*) is upregulated in activated blastocysts [13] and is downregulated during early myoblast differentiation, coincident with cell cycle withdrawal [14]. Targeted disruption of the Bysl gene in mouse results in embryonic lethality shortly after implantation [15]. These results collectively suggest that bystin plays a universal role in cell proliferation and that in higher organisms it has additional functions, some of which may be related to cell adhesion.

Recent DNA microarray data have revealed the expression patterns of bystin in multiple human cells and tissues (probe name for bystin, 203612_at; LSBM database, http://www.lsbm.org/site_e/database/index.html). A publicly available database shows that levels of bystin mRNA are relatively low in normal human tissues, consistent with a previous report [7], but expression of the bystin gene increases in cancer cells in various tumor types. Another microarrays analyzing surgical specimens of breast tumors have identified bystin in the “proliferation cluster” [16]. These observations prompted us to investigate bystin’s role in proliferation of cancer cells. Here we show that bystin in human cancer cells plays a role in ribosomal biogenesis, specifically in the processing of 18S rRNA to produce the 40S subunit.

EXPERIMENTAL

Antibodies

Polyclonal anti-bystin antibody was raised in rabbits against a synthetic peptide, MEKLTEKQTEVETVC (corresponding to human bystin amino acid residues 152-165) conjugated to keyhole limpet hemocyanin for immunization (the cysteine added for conjugation is underlined) [15]. For affinity purification, rabbit antiserum was absorbed on the antigen peptide linked to agarose beads prepared using SulfoLink coupling gel (Pierce Biotechnologies, Rockford, IL, USA), eluted with 0.2 M glycine-HCl, pH 2.4, and immediately neutralized with 1 M Tris-HCl, pH 8.5. The following antibodies were purchased: mouse monoclonal anti-FLAG tag antibody (M2) and anti-α tubulin antibody from Sigma (St Louis, MO, USA); mouse monoclonal anti-F_1F_0 ATP synthase (complex V) β subunit antibody from MitoSciences (Eugene, OR, USA); mouse monoclonal anti-fibrillarin antibody from EnCor Biotechnology (Alachua, FL, USA); rat monoclonal anti-HSF1 antibody from Upstate (Charlottesville, VA, USA); rabbit polyclonal anti-ribosomal protein L10/QM antibody (C-17) and from Santa Cruz Biotechnology (Santa Cruz, CA, USA); rabbit polyclonal anti-ribosomal protein S6 antibody and anti-phospho-S6 ribosomal protein (Ser240/244) antibody from Cell Signaling Technology (Danvers, MA, USA); and mouse monoclonal anti-SC35 antibody from BD Biosciences (San Jose, CA, USA).

Cell culture

Human cell lines of HeLa (cervical carcinoma), Jurkat (T-cell leukemia), MCF-7 (breast carcinoma), U-937 (monoblastic leukemia), YMB-1 (breast carcinoma), and 293T (embryonic kidney) were cultured at 37°C as described [8, 17].

For nucleolar stress experiments, HeLa cells were treated with 10 ng/ml (8.0 nM) actinomycin D (ActD, Sigma) (from a stock solution of 1.0 mg/ml in dimethyl sulfoxide) for 24 h. Control cells were treated with the same volume of vehicle. For heat shock, cells were treated at 42°C for 30 min. For treatment with rapamycin, cells

were incubated for 24 h with 20 nM rapamycin (dissolved in dimethyl sulfoxide; LC Laboratories, Woburn, MA, USA). Controls cells were treated with the same volume of dimethyl sulfoxide.

Plasmids and transfections

An IMAGE cDNA clone (accession no. BC050645; clone ID, 6011459), encoding 50-kDa bystin (accession no. NM_004053) [15], was identified by searching EST databases and obtained from Invitrogen (Carlsbad, CA, USA). The open reading frame was amplified by the polymerase chain reaction (PCR) using forward primer 5'-TTTGAATTCGAGAAAAATGCCCAAATTC-3' (*Eco* RI site underlined) and reverse primer 5'-TTTGGTACCTCCACGGTGATGGGAACA-3' (*Kpn* I site underlined) and inserted between *Eco* RI and *Kpn* I sites of pFLAG vector (Sigma) to overexpress C-terminally FLAG-tagged bystin in mammalian cells. Cells were transfected using Lipofectamine Plus (Invitrogen) according to the manufacturer's instructions.

Reverse transcription (RT)-PCR

Isolation of total RNA with Trizol reagent (Invitrogen), deoxyribonuclease I (Invitrogen) treatment, and RT using Superscipt II and an oligo$(dT)_{12\text{-}18}$ primer (Invitrogen) were described previously [18]. Partial cDNA (177 bp) of human bystin was amplified by PCR from the RT products as follows. PCR primers were: 5'-CTGGTTCAAAGGGATCCTGA-3' (forward) and 5'-AGTCGCAGGAAGATGCTGTT-3' (reverse). Amplification was carried out using rTaq DNA polymerase (Takara, Otsu, Japan) and the following protocol: denaturation at 94^{o}C for 4 min; 30 cycles of denaturation at 94^{o}C for 1min, annealing at 60^{o}C for 1 min; and extension at 72^{o}C for 1 min. Products were analyzed on agarose gels, isolated, and sequenced as described [18].

Immunoblotting

Proteins were separated by sodium dodecyl sulfate-polyacrylamide gel electrophoresis (SDS-PAGE), electroblotted onto Immobilon membranes (Millipore, Bedford, MA, USA), reacted first with primary antibodies and then with horseradish peroxidase-conjugated secondary antibodies, and detected using the ECL detection system (GE Healthcare Biosciences, Piscataway, NJ, USA) as described [17, 18], except for two modifications using the anti-bystin antibody. First, the Can-Get-Signal reagent (Toyobo, Osaka, Japan) was used to dilute primary and secondary antibodies. Also, horseradish peroxidase-conjugated mouse monoclonal antibody against rabbit immunoglobulin G (light chain specific; Jackson ImmunoResearch, West Grove, PA, USA) was used as the secondary antibody.

For peptide blocking experiments, anti-bystin antibody (2 μg) was mixed with immunogen peptide (8 μg in water) and incubated for 15 h at 4^{o}C. Controls were treated similarly with an unrelated peptide. Mixtures were centrifuged at 14,000 g for 15 min at 4^{o}C, and supernatants were subjected to immunoblotting.

Band intensities of immunoblots were evaluated by using an image analyzer (the Cool Saver AE-6955 detection system including the CS Analyzer software, Atto, Tokyo, Japan). Statistical analysis (two-sample *t*-test for independent samples) was conducted to evaluate expression levels.

Subcellular fractionation

All procedures were based on published methods [19]. Adherent cells in a 90-mm dish were harvested and washed with phosphate-buffered saline. Washed cells were suspended in 2 ml of 10 mM Tris-HCl, pH 7.4, containing 10 mM NaCl and 1.5 mM $MgCl_2$, kept on ice for 10 min, and homogenized with a glass Dounce homogenizer (tight fitting; Wheaton Science Products, Millville, NJ, USA). Homogenization was

verified by phase-contrast microscopy, phenylmethanesulfonyl fluoride (final concentration, 1 mM; Sigma) and phosphatase inhibitor cocktails 1 and 2 (Sigma) were added, and homogenates were centrifuged at 1,000 g for 3 min at 4°C. The nuclear fraction pellet was collected and the supernatant was centrifuged at 2,000 g for 30 min at 4°C. The second pellet (mitochondrial fraction plus lysosomes) was collected and the second supernatant was ultracentrifuged at 105,000 g for 60 min at 4°C, yielding the microsome/ribosome (P100) pellet and the cytoplasmic S100 supernatant. Proteins in the supernatant were precipitated with cold acetone (final concentration 80%). Fractions was boiled in SDS-PAGE sample buffer and immunoblotted.

Immunofluorescence

Cells on coverslips were fixed with cold methanol (-20^{o}C, 10 min) or paraformaldehyde and stained with primary antibodies and Alexa488- and Alexa568-conjugated secondary antibodies (Invitrogen) as described [8, 20]. Cells were observed under a confocal laser scanning microscope (LSM5 Pascal, Carl Zeiss, Jena, Germany). For peptide blocking experiments, anti-bystin antibody was treated with the peptide used as immunogen or with irrelevant peptides before cell staining, as in a similar manner as have done for immunoblotting.

Ribosome analysis

Total cytoplasmic ribosomes were isolated according to previous reports [17, 21] with modifications. Cells in ten 90-mm dishes were cultured for 10 min in the presence of 5 μg/ml cycloheximide (Sigma), harvested, washed with phosphate-buffered saline, and lysed for 15 min on ice with 2.5 ml of buffer C (20 mM Tris-HCl, pH 7.5, containing 0.1 M KCl, 5 mM $MgCl_2$, 10 mM 2-mercaptoethanol, and 10 μg/ml cycloheximide), to which was added 1% Triton X-100, 0.25 M sucrose, 1 mM phenylmethylsulfonyl fluoride, and 100 U/ml human placental ribonuclease inhibitor (Wako). Lysates were

centrifuged at 15,000 g for 10 min to collect the post-mitochondrial supernatants. Ultracentrifuge tubes (model no. 349622; Beckman, Palo Alto, CA, USA) were filled with 1.4 ml of buffer C containing 1.0 M sucrose. The post-mitochondrial supernatants (no more than 1.4 ml per tube) were added as the top layer. Tubes were centrifuged 22 h at 250,000 g at 4°C. Pellets were washed briefly with 5 mM Tris-HCl, pH 7.5, containing 50 mM KCl and 1.5 mM $MgCl_2$ and suspended in the same buffer. The concentration of isolated ribosomes was determined as described [21].

Isolated ribosomes (about 1.2 mg per tube) were layered onto linear gradients of 15-30% sucrose in buffer C in ultracentrifugation tubes (model no. 344059, Beckman) and ultracentrifuged in the SW41Ti swinging bucket rotor (Beckman) at 37,000 rpm for 3 h at 4°C. Gradients were analyzed by passing the contents through the single path UV-1 optical unit (GE Healthcare Biosciences) connected to a REC-482 chart recorder (GE Healthcare Biosciences) to monitor absorbance at 254 nm. 0.5 ml fractions were collected, and proteins in fractions were precipitated by trichloroacetic acid (final concentration, 10%), washed with cold ethanol, boiled in SDS-PAGE sample buffer, and immunoblotted.

RNA interference (RNAi)

Small interfering RNA (siRNA) duplex, siBys-D, designed and synthesized by iGene (Tsukuba, Japan), was targeted to the following sequence of human bystin cDNA: 5'-CCATAGAGATGTTCATGAACAAGAA-3'. siRNA duplex, siBys-G, designed and synthesized by B-Bridge International (Mountain View, CA, USA), was targeted to the following sequence of human bystin cDNA: 5'- CGAAATCAGGCGTGAGCTT -3'. As control duplex RNA, siLuc (iGene) corresponding to nucleotides 509-533 of firefly luciferase cDNA (accession no. M15077) was used. AG and UA 3' overhangs were added to sense and antisense duplex strands, respectively, in siBys-D and siLuc. TT 3' overhangs were added to both duplex strands in siBys-G. Duplexes were dissolved at

50 μM in ribonuclease-free water, aliquoted, and stored at -80°C until use.

For transfection, cells were cultured in six-well plates in antibiotic-free medium. Opti-MEM (Invitrogen) was warmed at 37°C before use. siRNA duplexes (1 μl) were diluted into 180 μl Opti-MEM in a 1.5-ml tube. In another tube, 4 μl Oligofectamine (Invitrogen) was added to 16 μl Opti-MEM and incubated for 5 min at room temperature. Solutions were mixed and incubated for 20 min at room temperature. After changing the medium to Opti-MEM (0.8 ml per well), Opti-MEM (200 μl) was combined with the mixture, added to cells, and incubated for 4 h. Finally, cells were cultured in normal medium.

Pulse-chase analysis of rRNA processing

Cells in six-well plates were pre-incubated in methionine-free medium for 15 min at 37°C and pulse-labeled with 50 μCi/ml [methyl-^{3}H] methionine [22] purchased from GE Healthcare Biosciences for 30 min. Chase was initiated by a change to medium with 150 μg/ml unlabelled methionine. At chase time points, total RNA was isolated from cells using Trizol and quantitated by absorbance at 260 nm. RNA (2.5 μg per lane) was separated on polyacrylamide-agarose composite gels as described [23], with modifications: (i) 0.1% *N,N′*-diallyltartardiamide (Avocado Organics, Karlsruhe, Germany) was added to a 29% acrylamide/1% *N,N′*-methylenebisacrylamide stock solution to increase gel stability [24] and (ii) gels were composed of 1.5% polyacrylamide and 0.7% agarose. Gels were then immersed in En^{3}Hance (NEN/PerkinElmer, Wellesley, MA, USA) for 60 min and then in cold 1% glycerol for 60 min, placed on Whatman 3MM CHR paper, dried at room temperature, and exposed to X-OMAT film (Kodak, Rochester, NY, USA) for seven days at -80 °C.

Effects of RNAi on cell proliferation

HeLa cells grown in a six-wells plate were transfected with siRNA duplexes (final

concentration, 50 nM) as described above, and cultured for 96 h in normal medium. Toxic duplex, siTox (siCONTROL TOX Transfection Control, [25]), was purchased from Dharmacon (Lafayette, CO, USA), and transfected in the same manner, except that the final duplex concentration was 100 nM [25], to evaluate transfection efficiency. After washing with phosphate-buffered saline, adherent cells were trypsinized, and numbers were counted by using a hematocytometer. The data were statistically evaluated by the two-sample *t*-test.

RESULTS

Expression of bystin in human cancer cell lines

DNA microarrays indicate that bystin is overexpressed in human cancer cell lines. To confirm this, total RNAs were collected from a transformed human embryonic kidney epithelia line, 293T, and spontaneous human cancer cell lines, including three lines of adherent cells (HeLa, MCF-7, and YMB-1) and two lines of non-adherent cells (Jurkat and U-937). As shown in Fig. 1A, bystin expression was confirmed by RT-PCR. Sequencing of the PCR products confirmed the expected amplification of bystin (data not shown).

Expression of bystin protein was determined by immunoblotting with affinity-purified anti-bystin antibody, which indicated that all cell lines expressed a specific 50-kDa protein (Fig. 1B), an observation consistent with the calculated molecular mass, 49.6 kDa, of full-length human bystin, which is composed of 437 amino acids [15]. Although human bystin was originally reported to be a protein with 306 amino acids, subsequent study revealed that this was a truncated form [11]. When a vector harboring C-terminally FLAG-tagged bystin was transiently transfected into HeLa cells, overexpressed protein showed mobility close to 50 kDa (left blot of Fig. 1C). Furthermore, reactivity of the anti-bystin antibody with the 50-kDa band was

blocked by pre-treatment of the antibody with the immunogen peptide (right blot of Fig. 1C). Therefore, the 50-kDa band detected by the anti-bystin antibody is likely to be human bystin protein. Our data support the observation that bystin is overexpressed in various human cancer cells.

Endogenous bystin in HeLa cells localizes to the nucleus and cytoplasm

Previous observations indicate that bystin protein is primarily cytoplasmic in trophoblastic and placental cells [7, 26]. We chose HeLa cells to determine bystin localization in human cancer cells, since this line apparently expresses no active trophinin: DNA microarrays indicate that trophinin expression level is low (probe name for trophinin, 211700_s_at; LSBM database) and apical and homophilic cell adhesion characteristic of trophinin-mediated adhesion is not seen in this line [5].

HeLa cells were lysed and fractionated by differential centrifugation (Fig. 2, lanes 1-4). Successful fractionation was confirmed using appropriate markers. Bystin was clearly detected in nuclei and in the P100 and cytoplasmic S100 fractions. Similar localization was observed in 293T cells (Fig. 2, lanes 5-8). Occasionally, bystin reactivity was seen as multiple bands (Fig. 2, lanes 4 and 8), possibly due to partial degradation occurring during fractionation. Nonetheless, the results (Fig. 2) suggest that bystin proteins localize to the cytoplasm and nuclei of HeLa cells.

Nuclear bystin is present primarily in the nucleolus

To further analyze bystin localization, immunofluorescence using anti-bystin antibody was performed. HeLa cells were fixed with cold methanol and stained with the anti-bystin antibody. Strong positive signals were detected within the nucleus and weak signals was detected in the cytoplasm (Fig. 3A). These positive signals disappeared by pretreatment of the anti-bystin antibody with the immunogenic peptide, which supports specific reactivity of this antibody in immunofluorescence (Fig. 3C).

Staining patterns were similar when cells were fixed with paraformaldehyde (data not shown). Although association of bystin with cytoskeratin has been observed in other cell types [7], no filamentous structure suggestive of an association of bystin with cytokeratin was detected in HeLa cells.

Under normal culture conditions, bystin was seen in large globular structures in the nucleus, in addition to uniform staining in the nucleoplasm. To identify the globular structures, double immunostaining with anti-bystin antibodies and antibodies for the nucleolar marker fibrillarin/Nop1 and the marker for speckles, SC35, (Fig. 3B) was undertaken. Fibrillarin is included in nuclear substructures of the nucleolus [27], while speckles, including those positive for SC35, are sites of mRNA splicing [28]. Bystin colocalized with fibrillarin, but not with SC35, indicating that bystin is mainly located in the nucleolus, a finding consistent with proteomics analysis of nucleolar proteins [29].

Some extranuclear bystin associates with the ribosomal 40S subunit but not with the 80S monosome or polysomes

Bystin was detected in the nucleolus (Fig. 3B), whose main function is ribosome biogenesis [27]. Subcellular fractionation also showed co-sedimentation of bystin with the ribosomal S6 protein (Fig. 2). Hence, we asked whether bystin associates with ribosomes. Total cytoplasmic ribosomes were collected from a HeLa cell lysate and fractionated by sucrose-gradient ultracentrifugation (Fig. 4). Each fraction was examined for bystin, S6 as part of the 40S subunit, and L10 as part of the 60S subunit. In addition to being found monosome and polysome fractions, S6 and L10 were present in fractions of 40S and 60S subunits, respectively, confirming successful fractionation. Bystin was detected in fractions including 40S subunits but not in other ribosomal fractions, including those containing actively translating polysomes. These results suggest that in HeLa cells bystin protein is included in the 40S subunit in the cytoplasm

but dissociates from the subunit before initiation of translation.

Bystin knockdown causes a delay in rRNA processing and inhibited cell proliferation

Studies of budding yeast indicate that ribosome biogenesis begins in the nucleolus and that precursors of the 40S and 60S subunits are separately exported from the nucleus through nuclear pores [30]. Maturation of the 40S subunit, including final processing of 18S rRNA, occurs in the cytoplasm both in yeast [30] and HeLa cells [31]. The finding that bystin is present in the nucleolus and associates with the 40S subunit, probably with cytoplasmic pre-40S particles [31], suggests that it functions in biosynthesis. To test this hypothesis, RNAi was used to evaluate effects of its loss of function.

Six siRNAs were designed and transiently introduced into HeLa cells by lipofection. Bystin protein levels were examined by immunoblotting, which showed that siBys-D and siBys-G suppressed expression of bystin protein (Fig. 5A). Relatively constant expression of α-tubulin after transfection with siBys-D and siBys-G or bystin after transfection of control Luc siRNA indicated that effects of siBys-D and siBys-G were specific.

rRNAs precursors are processed and modified in the nucleolus [30, 32]. The effect of bystin RNAi on rRNA processing was evaluated by pulse-chase analysis of ribosomal components (Fig. 5B). In HeLa cells, 5.8S , 18S, and 28S rRNAs are generated from a 45S transcript via two pathways (Fig. 5C) [33]. In samples from cells transfected with siBys-D or siBys-G, a band intermediate in size between 18S and 28S rRNAs was intensified in each panel (arrows, Fig. 5B). Among the intermediates observed (Fig. 5C), a 21S rRNA product accumulated between 18S and 28S rRNAs in these. Because 21S rRNA is a precursor of 18S rRNA in either of the two alternative pathways, bystin may function in processing of the 18S rRNA in the 40S subunit.

Since ribosome biogenesis is important factor for cancer cell growth [34], effects of bystin siRNA on viability of HeLa cells were evaluated. Knockdown of bystin by siBys-D and siBys-G significantly reduced cell proliferation (Fig. 5D). Collectively, our data suggest that bystin promotes cell proliferation by facilitating ribosome biogenesis, specifically in the production of the 40S subunit.

Bystin disappears from the nucleolus under nucleolar stress, while free or cytosolic bystin is unaffected

If bystin functions in rRNA processing, its localization may change when ribosome biogenesis is inhibited. The initial 45S pre-rRNA is transcribed from repetitive rDNAs by RNA polymerase I in the nucleolus [27]. To determine the relationship between bystin and ribosome biogenesis, we employed so-called nucleolar stress mediated by ActD, which at low levels selectively inhibits RNA polymerase I [35, 36].

As described [37], treatment of HeLa cells with ActD caused shrinkage of nucleoli as visualized by the marker protein, fibrillarin (Fig. 6A). Under these stress conditions, bystin was not detected in the nucleolus. To confirm this observation biochemically, bystin levels were determined by immunoblotting after subcellular fractionation (Fig. 6B). No bystin was detected from nuclear or P100 fractions under nucleolar stress conditions, whereas other marker proteins, including fibrillarin and ribosomal protein S6, remained in these fractions. The apparently specific disappearance of bystin suggests a rapid response to the state of ribosome biogenesis. By contrast, bystin levels in the S100 (cytosol) fraction were relatively constant under these conditions.

To monitor localization of bystin proteins associated with ribosome biogenesis, C-terminally FLAG-tagged bystin protein was overexpressed in HeLa cells, and cells were treated with ActD. Without treatment, bystin-FLAG localized mainly to the nucleolus (bottom panels of Fig. 7A). Under stress conditions, bystin-FLAG was not

detected in the segregated nucleolus and instead formed particle-like structures in the nucleoplasm (arrows, top panel of Fig. 7A).

Nuclear stress-induced granules that include HSF1 have been reported in other stress conditions, such as heat shock [38]. Under heat shock conditions, endogenous bystin localization was unchanged, nor did bystin colocalize with HSF1 (Fig. 7B). Also under nucleolar stress conditions, bystin-FLAG did not colocalize with HSF1: bystin-FLAG was seen as small nuclear particles but HSF1 was spread throughout nuclei (Fig. 7C). These results suggest the following conclusions: (i) under nucleolar stress, bystin is rapidly released from the nucleolus and moves to small particles within the nucleus; (ii) particles including bystin are specific to nucleolar stress; and (iii) bystin-containing particles differ from nuclear stress-induced and HSF1-containing granules.

The mammalian target of rapamycin (mTOR) may regulate bysin expression in cancer cells

Ribosome biogenesis is dependent on mTOR activity, which is induced by growth factors and nutrients [39, 40]. To find a link between mTOR and bystin, effects of inhibition of mTOR in cancer cells were examined using rapamycin. Phosphorylation of ribosomal protein S6 has been reported to be stimulated by mTOR [41]. Our data indicated that the levels of phosphorylated S6 were reduced in rapamycin-treated HeLa cells and 293T cells (Fig. 8A). The expression of bystin was also significantly reduced by the rapamycin treatment (Fig. 8B). Similar reduction was detected for a nucleolar protein involved in ribosome biogenesis, fibrillarin, and a ribosomal component, S6.

The immunoblotting data (Fig. 8) support the involvement of bystin in ribosome biogenesis. However, comparing the prominent effect of TOR on rRNA transcription by RNA polymerase I demonstrated in yeast and mammalian cells [40], the effects of rapamycin on bystin, fibrillarin and ribosomal S6 (Fig. 8B) are somewhat

weak. In the previous study by others, expression of genes of ribosomal proteins in yeast is determined at the transcriptional level using TOR [39], whereas these genes in higher eukaryotes are under both transcriptional and translational controls [41, 42]. Nonetheless, our data suggest that bystin is likely involved in the mTOR signaling pathway.

DISCUSSION

The process of ribosomal biogenesis differs significantly between prokaryotes and eukaryotes despite functional conservation of the ribosome in protein synthesis. In eubacteria, the ribosome can self-assemble and be reconstituted *in vitro* [43]. In budding yeast, ribosome synthesis is assisted by more than 150 non-ribosomal proteins, many of which are essential for growth [30, 44]. These non-ribosomal factors have homologues in other species, and some share properties with mammalian pre-ribosomal complexes [32]. Some human factors, including fibrillarin [45], can complement, at least partially, yeast strains with mutations in their orthologues. Hence, an elaborate system for biogenesis is likely conserved in eukaryotes, including humans. Recent studies show that cancer progression depends on ribosome biogenesis. For example, pathways in ribosome synthesis are regulated by the well-known tumor suppressors, pRb and p53 [34]. Compounds like rapamycin, which are known to inhibit ribosome biogenesis and translation initiation, are recognized as effective anticancer drugs [46]. Therefore, defining factors and pathways involved in ribosome biogenesis is of strategic importance for cancer therapy. Just as many antibiotics interfere with the formation of the prokaryotic ribosome [47], biogenesis of the human ribosome could be a good target to antagonize malignant neoplasms.

Several lines of evidence presented here indicate that bystin functions in

ribosome biogenesis in human cells. (i) Bystin is located in the nucleolus, the organelle where ribosomal biogenesis takes place (Fig. 3). (ii) Bystin is associated with the cytoplasmic 40S subunit, a component of the 80S monosome, before translation is initiated (Fig. 4). (iii) Down-regulation of bystin delays processing of the 18S rRNA or mature form required for protein translation, which resulted in compromised cell viability (Fig. 5). (iv) Inhibition of mTOR activity suppressed the expression of bystin (Fig. 8). Furthermore, nucleolar bystin and bystin associated with the 40S subunit both disappear under conditions of nucleolar stress (Fig. 6), suggesting that bystin in both locations is functionally linked. Bystin may be associated with a precursor of the 40S subunit—a pre-40S particle—in the nucleolus and exported with these particles through nuclear pores, where it dissociates from particles in the cytoplasm at very late phases of subunit synthesis, as has been shown by Enp1 studies [48]. Given the dependence of cancer cell growth on ribosome biogenesis, high expression of bystin in cancer cells (Fig. 1) may contribute to proliferation, a hypothesis supported by the fact that the bystin gene is amplified in diffuse large B-cell lymphoma [49].

Although bystin exhibits activities similar to Enp1 [11, 48], Enp1-null yeast mutant phenotypes cannot be complemented with human bystin [11]. rRNA processing pathways in multicellular organisms reportedly diverge from those seen in yeast [50], and bystin's precise activity across species has likely been modified in the course of evolution. In higher organisms, at very early developmental stages, embryos grow rapidly after implantation, and speedy synthesis of the primary translational machinery, the ribosome, is required. Nonetheless, evidence linking ribosome biogenesis with early development has been sparse until now. Our data, together with distribution of fly Bys in proliferative embryonic tissues [9] and upregulation of the mouse bystin homologue in activated blastocysts [13] and the epiblast [15] support a role for bystin in ribosome biogenesis. Comparing the activities of bystin orthologues

may identify species-specific functions of bystin family members in rRNA processing and new regulatory mechanisms in ribosome biogenesis.

We found biochemically a substantial amount of cytoplasmic bystin protein in HeLa cells (Fig. 2). Thus paradoxical weak immunostaining of cytoplasmic bystin (Fig. 3A) may be caused by two reasons: (i) the epitope recognized by anti-bystin antibody may be inaccessible when bystin is associated with the 40S subunit (Fig. 4) and (ii) bystin not associated with the 40S subunit may be diluted in a large cytoplasmic region. Cytoplasmic localization of bystin contrasts to the almost exclusively nuclear localization of Enp1 seen in yeast cells [11, 48, 51]. Comprehensive proteomics analysis of yeast nuclear proteins shows that nuclear proteins are not stored in the cytoplasm [48, 51]. It is known that newly synthesized ribosomal proteins in the cytoplasm are immediately transported to the nucleolus ([20] and references therein). Indeed, no cytoplasmic pool was detected for nucleolar fibrillarin and ribosomal S6 in this study (Fig. 2, lanes 4 and 8). Thus, bystin's cytoplasmic localization far from the nucleolus may be unique. Because bystin expression levels in the cytosol (S100 fraction) were unchanged following ActD treatment (compare lanes 4 and 8 in Fig. 6B), cytosolic bystin may play a role other than ribosomal biogenesis. Previously, it was shown that bystin functions in cell adhesion during human embryo implantation [7, 26]. Also in prostate cancer, bystin was found in prostate cancer cells adhering to neuronal cells [52]. *Drosophila* Bys mRNA has been reported to be expressed in a pattern suggesting a role in cell-cell contact [9]. The precise function of cytoplasmic bystin thus awaits further investigation.

We also show bystin in undefined nuclear particles following ActD treatment (Fig. 7). Although these particles were observed under overexpression conditions, nucleolar stress-induced particles appear specific to bystin. Because there are no membrane boundaries within the nucleus, factors can be exchanged dynamically. As nuclear stress-granules can serve as storage sites for transcription factors [38], factors

used in ribosome biogenesis shuttle between the nucleolus and nucleoplasm [30]. Given the dependence of cell proliferation on ribosome biogenesis, when biogenesis is halted by nucleolar stress, this system may allow rapid resynthesis upon release from stress. Proteomic analysis of particles including tagged-bystin may identify their contents, as has been shown with other nuclear particles [29, 53]. Currently, the mechanism underlying such trafficking of bystin under nucleolar stress is unknown.

In summary, we show that bystin likely functions in ribosome biogenesis through 18S rRNA processing in mammalian cells. Given that ribosome biogenesis is coupled to cellular growth, the idea that bystin is upregulated in cancer cells is logical. Further analysis of bystin together with Enp1 and Bys should provide new insight for understanding bystin function across species and may also suggest therapeutic strategies against cancer.

Acknowledgments

This study was supported by research grants from NOVARTIS Foundation (Japan) for the Promotion of Science, the Sagawa Foundation for Promotion of Cancer Research, the Sumitomo Foundation, and Towa Shokuhin, and in part by a grant-in-aid for Scientific Research from the Ministry of Education, Culture, Sports, Science and Technology of Japan, and Department of Defense, Prostate Cancer Research Program IDEA grant W81XWH-04-1-0917 (to MNF).

REFERENCES

1. Carson, D.D., Bagchi, I., Dey, S.K., Enders, A.C., Fazleabas, A.T., Lessey, B.A. and Yoshinaga, K. (2000) Embryo implantation. Dev. Biol. **223**, 217-237
2. Cross, J.C., Werb, Z. and Fisher, S.J. (1994) Implantation and the placenta: key

pieces of the development puzzle. Science **266**, 1508-1518

3. Strickland, S. and Richards, W.G. (1992) Invasion of the trophoblasts. Cell **71**, 355-357
4. Murray, M.J. and Lessey, B.A. (1999) Embryo implantation and tumor metastasis: common pathways of invasion and angiogenesis. Semin. Reprod. Endocrinol. **17**, 275-290
5. Fukuda, M.N., Sato, T., Nakayama, J., Klier, G., Mikami, M., Aoki, D. and Nozawa, S. (1995) Trophinin and tastin, a novel cell adhesion molecule complex with potential involvement in embryo implantation. Genes Dev. **9**, 1199-1210
6. Hatakeyama, S., Ohyama, C., Minagawa, S., Inoue, T., Kakinuma, H., Kyan, A., Arai, Y., Suga, T., Nakayama, J., Kato, T., Habuchi, T. and Fukuda, M.N. (2004) Functional correlation of trophinin expression with the malignancy of testicular germ cell tumor. Cancer Res. **64**, 4257-4262
7. Suzuki, N., Zara, J., Sato, T., Ong, E., Bakhiet, N., Oshima, R.G., Watson, K.L. and Fukuda, M.N. (1998) A cytoplasmic protein, bystin, interacts with trophinin, tastin, and cytokeratin and may be involved in trophinin-mediated cell adhesion between trophoblast and endometrial epithelial cells. Proc. Natl. Acad. Sci. USA **95**, 5027-5032
8. Nadano, D., Nakayama, J., Matsuzawa, S., Sato, T., Matsuda, T. and Fukuda, M.N. (2002) Human tastin, a proline-rich cytoplasmic protein, associates with the microtubular cytoskeleton. Biochem. J. **364**, 669-677
9. Stewart, M.J. and Nordquist, E.K. (2005) Drosophila Bys is nuclear and shows dynamic tissue-specific expression during development. Dev. Genes Evol. **215**, 97-102
10. Roos, J., Luz, J.M., Centoducati, S., Sternglanz, R. and Lennarz, W.J. (1997) ENP1, an essential gene encoding a nuclear protein that is highly conserved from yeast to humans. Gene **185**, 137-146

11. Chen, W., Bucaria, J., Band, D.A., Sutton, A. and Sternglanz, R. (2003) Enp1, a yeast protein associated with U3 and U14 snoRNAs, is required for pre-rRNA processing and 40S subunit synthesis. Nucleic Acids Res. **31**, 690-699

12. Basso, K., Margolin, A.A., Stolovitzky, G., Klein, U., Dalla-Favera, R. and Califano, A. (2005) Reverse engineering of regulatory networks in human B cells. Nat. Genet. **37**, 382-390

13. Hamatani, T., Daikoku, T., Wang, H., Matsumoto, H., Carter, M.G., Ko, M.S. and Dey, S.K. (2004) Global gene expression analysis identifies molecular pathways distinguishing blastocyst dormancy and activation. Proc. Natl. Acad. Sci. USA **101**, 10326-10331

14. Shen, X., Collier, J.M., Hlaing, M., Zhang, L., Delshad, E.H., Bristow, J. and Bernstein, H.S. (2003) Genome-wide examination of myoblast cell cycle withdrawal during differentiation. Dev. Dyn. **226**, 128-138

15. Aoki, R., Suzuki, N., Paria, B.C., Sugihara, K., Akama, T.O., Raab, G., Miyoshi, M., Nadano, D. and Fukuda, M.N. (2006) The *Bysl* gene product, bystin, is essential for survival of mouse embryos. FEBS Lett. **580**, 6062-6068

16. Perou, C.M., Sorlie, T., Eisen, M.B., van de Rijn, M., Jeffrey, S.S., Rees, C.A., Pollack, J.R., Ross, D.T., Johnsen, H., Akslen, L.A., Fluge, O., Pergamenschikov, A., Williams, C., Zhu, S.X., Lonning, P.E., Borresen-Dale, A.L., Brown, P.O. and Botstein, D. (2000) Molecular portraits of human breast tumours. Nature **406**, 747-752

17. Nadano, D., Aoki, C., Yoshinaka, T., Irie, S. and Sato, T. (2001) Electrophoretic characterization of ribosomal subunits and proteins in apoptosis: specific down-regulation of S11 in staurosporine-treated human breast carcinoma cells. Biochemistry **40**, 15184-15193

18. Nakamura, M., Tomita, A., Nakatani, H., Matsuda, T. and Nadano, D. (2006) Antioxidant and antibacterial genes are upregulated in early involution of the

mouse mammary gland: sharp increase of ceruloplasmin and lactoferrin in accumulating breast milk. DNA Cell Biol. **25**, 491-500

19. Pederson, T. (1998) Preparation of nuclei from tissue and suspension cultures. In *Cells: A Laboratory Manual*, Volume 1 (D. L. Spector, R. D. Goldman and L. A. Leinwand, eds), Cold Spring Harbor Laboratory Press, New York 43.1-43.14
20. Nadano, D., Notsu, T., Matsuda, T. and Sato, T. (2002) A human gene encoding a protein homologous to ribosomal protein L39 is normally expressed in the testis and derepressed in multiple cancer cells. Biochim. Biophys. Acta **1577**, 430-436
21. Nadano, D., Ishihara, G., Aoki, C., Yoshinaka, T., Irie, S. and Sato, T. (2000) Preparation and characterization of antibodies against human ribosomal proteins: heterogeneous expression of S11 and S30 in a panel of human cancer cell lines. Jpn. J. Cancer Res. **91**, 802-810
22. Udem, S.A. and Warner, J.R. (1972) Ribosomal RNA synthesis in Saccharomyces cerevisiae. J. Mol. Biol. **65**, 227-242
23. Nadano, D. and Sato, T. (2000) Caspase-3-dependent and -independent degradation of 28 S ribosomal RNA may be involved in the inhibition of protein synthesis during apoptosis initiated by death receptor engagement. J. Biol. Chem. **275**, 13967-13973
24. Baumann, G. and Chrambach, A. (1976) A highly crosslinked, transparent polyacrylamide gel with improved mechanical stability for use in isoelectric focusing and isotachophoresis. Anal. Biochem. **70**, 32-38
25. Reynolds, A., Anderson, E.M., Vermeulen, A., Fedorov, Y., Robinson, K., Leake, D., Karpilow, J., Marshall, W.S. and Khvorova, A. (2006) Induction of the interferon response by siRNA is cell type- and duplex length-dependent. RNA **12**, 988-993
26. Suzuki, N., Nakayama, J., Shih, I.-M., Aoki, D., Nozawa, S. and Fukuda, M.N.

(1999) Expression of trophinin, tastin, and bystin by trophoblast and endometrial cells in human placenta. Biol. Reprod. **60**, 621-627

27. Maggi, L.B., Jr and Weber, J.D. (2005) Nucleolar adaptation in human cancer. Cancer Invest. **23**, 599-608

28. Spector, D.L. (2001) Nuclear domains. J. Cell Sci. **114**, 2891-2893

29. Andersen, J.S., Lyon, C.E., Fox, A.H., Leung, A.K., Lam, Y.W., Steen, H., Mann, M. and Lamond, A.I. (2002) Directed proteomic analysis of the human nucleolus. Curr. Biol. **12**, 1-11

30. Dez, C. and Tollervey, D. (2004) Ribosome synthesis meets the cell cycle. Curr. Opin. Microbiol. **7**, 631-637

31. Rouquette, J., Choesmel, V. and Gleizes, P.E. (2005) Nuclear export and cytoplasmic processing of precursors to the 40S ribosomal subunits in mammalian cells. EMBO J. **24**, 2862-2872

32. Takahashi, N., Yanagida, M., Fujiyama, S., Hayano, T. and Isobe, T. (2003) Proteomic snapshot analyses of preribosomal ribonucleoprotein complexes formed at various stages of ribosome biogenesis in yeast and mammalian cells. Mass Spectrom. Rev. **22**, 287-317

33. Hadjiolova, K., Nicoloso, M., Mazan, S., Hadjiolov, A.A. and Bachellerie, J.P. (1993) Alternative pre-rRNA processing pathways in human cells and their alteration by cycloheximide inhibition of protein synthesis. Eur. J. Biochem. **212**, 211-215

34. Ruggero, D. and Pandolfi, P.P. (2003) Does the ribosome translate cancer? Nat. Rev. Cancer **3**, 179-192

35. Pestov, D.G., Strezoska, Z. and Lau, L.F. (2001) Evidence of p53-dependent cross-talk between ribosome biogenesis and the cell cycle: effects of nucleolar protein Bop1 on G(1)/S transition. Mol. Cell. Biol. **21**, 4246-4255

36. Lohrum, M.A.E., Ludwig, R.L., Kubbutat, M.H.G., Hanlon, M. and Vousden,

K.H. (2003) Regulation of HDM2 activity by the ribosomal protein L11. Cancer Cell **3**, 577-587

37. Yokoyama, Y., Niwa, K. and Tamaya, T. (1992) Scattering of the silver-stained proteins of nucleolar organizer regions in Ishikawa cells by actinomycin D. Exp. Cell Res. **202**, 77-86
38. Sandqvist, A. and Sistonen, L. (2004) Nuclear stress granules: the awakening of a sleeping beauty? J. Cell Biol. **164**, 15-17
39. Arsham, A.M. and Neufeld, T.P. (2006) Thinking globally and acting locally with TOR. Curr. Opin. Cell Biol. **18**, 589-597
40. Mayer, C. and Grummt, I. (2006) Ribosome biogenesis and cell growth: mTOR coordinates transcription by all three classes of nuclear RNA polymerases. Oncogene **25**, 6384-6391
41. Thomas, G. and Hall, M.N. (1997) TOR signalling and control of cell growth. Curr. Opin. Cell Biol. **9**, 782-787
42. Mager, W.H. (1988) Control of ribosomal protein gene expression. Biochim. Biophys. Acta **949**, 1-15
43. Nomura, M. (1973) Assembly of bacterial ribosomes. Science **179**, 864-873
44. Warner, J.R. (2001) Nascent ribosomes. Cell **107**, 133-136
45. Jansen, R.P., Hurt, E.C., Kern, H., Lehtonen, H., Carmo-Fonseca, M., Lapeyre, B. and Tollervey, D. (1991) Evolutionary conservation of the human nucleolar protein fibrillarin and its functional expression in yeast. J. Cell Biol. **113**, 715-729
46. Pandolfi, P.P. (2004) Aberrant mRNA translation in cancer pathogenesis: an old concept revisited comes finally of age. Oncogene **23**, 3134-3137
47. Champney, W.S. (2003) Bacterial ribosomal subunit assembly is an antibiotic target. Curr. Top. Med. Chem. **3**, 929-947
48. Schafer, T., Strauss, D., Petfalski, E., Tollervey, D. and Hurt, E. (2003) The path

from nucleolar 90S to cytoplasmic 40S pre-ribosomes. EMBO J. **22**, 1370-1380

49. Kasugai, Y., Tagawa, H., Kameoka, Y., Morishima, Y., Nakamura, S. and Seto, M. (2005) Identification of *CCND3* and *BYSL* as candidate targets for the 6p21 amplification in diffuse large B-cell lymphoma. Clin. Cancer Res. **11**, 8265-8272

50. Gerbi, S.A. and Borovjagin, A.V. (2004) Pre-ribosomal RNA processing in multicellular organisms. In *The Nucleolus* (M. O. J. Olson, ed) Kluwer Academic, New York 170-198

51. Grandi, P., Rybin, V., Bassler, J., Petfalski, E., Strauss, D., Marzioch, M., Schafer, T., Kuster, B., Tschochner, H., Tollervey, D., Gavin, A.C. and Hurt, E. (2002) 90S pre-ribosomes include the 35S pre-rRNA, the U3 snoRNP, and 40S subunit processing factors but predominantly lack 60S synthesis factors. Mol. Cell **10**, 105-115

52. Ayala, G.E., Dai, H., Li, R., Ittmann, M., Thompson, T.C., Rowley, D. and Wheeler, T.M. (2005) Bystin in perineural invasion of prostate cancer. Prostate **66**, 266-272

53. Gavin, A.C., Bosche, M., Krause, R., Grandi, P., Marzioch, M., Bauer, A., Schultz, J., Rick, J.M., Michon, A.M., Cruciat, C.M., Remor, M., Hofert, C., Schelder, M., Brajenovic, M., Ruffner, H., Merino, A., Klein, K., Hudak, M., Dickson, D., Rudi, T., Gnau, V., Bauch, A., Bastuck, S., Huhse, B., Leutwein, C., Heurtier, M.A., Copley, R.R., Edelmann, A., Querfurth, E., Rybin, V., Drewes, G., Raida, M., Bouwmeester, T., Bork, P., Seraphin, B., Kuster, B., Neubauer, G. and Superti-Furga, G. (2002) Functional organization of the yeast proteome by systematic analysis of protein complexes. Nature **415**, 141-147

Figure Legends

Figure 1 Expression of bystin in human cell lines

(A) RT-PCR analysis of bystin mRNA. cDNAs were prepared by reverse transcription (RT) of RNA from the indicated human cell lines, amplified by PCR with primers designed from bystin cDNA, and analyzed by electrophoresis. +, plus reverse transcriptase; -, without reverse transcriptase. (B) Immunoblot analysis of bystin protein. Lysates of cells indicated were immunoblotted with affinity purified anti-bystin antibody. Band corresponding to putative bystin protein is indicated by arrow. (C) Immunoblotting of FLAG-tagged bystin. HeLa cells were transiently transfected with mock DNA (lane 1) and an expression vector for bystin-FLAG (lane 2) and immunoblotted with the anti-bystin antibody. The antibody was treated with the immunogenic (immuno.) peptide (right blot) or with control peptide (left blot) before use. In (B) and (C), proteins from about 1 X 10^5 cells were loaded into each well and separated in 10% polyacrylamide gels.

Figure 2 Bystin protein in nuclei, ribosomes, and cytoplasmic fractions

HeLa (lanes 1-4) and 293T (lanes 5-8) cells were subjected to subcellular fractionation as indicated (see Experimental). Each fraction was analyzed by immunoblotting with the antibodies indicated on the right. Markers used were fibrillarin for nuclei (nuc.), F_1F_0 ATP synthase (complex V) β subunit for mitochondria (mito.), ribosomal protein S6 for P100, and α-tubulin for cytoplasmic S100.

Figure 3 Localization of bystin in the nucleolus

(A) HeLa cells were double-immunostained with antibodies against bystin (red) and α-tubulin (green). Note that bystin is detected in large nuclear particles (arrows, left panel). (B) (top panels) HeLa cells were double-immunostained with antibodies

against bystin (red) and the nucleolar marker fibrillarin (green). Bystin immunostaining in merged image overlaps with that of fibrillarin. (bottom panels) By contrast, in cells stained for bystin (red) and the nuclear speckle marker SC53 (green), staining does not overlap. (C) Anti-bystin antibody was treated with the immunogenic (immuno.) peptide or with control peptide prior to use for cell staining. The staining patterns obtained with the anti-bystin antibody disappeared by preincubation of the antibody with the immunogenic peptide, but not with the unrelated peptide. DIC, differential interference contrast; bars, 5 μm.

Figure 4 Bystin in ribosomal fractions

(upper panel) Total cytoplasmic ribosomes (from lysates of HeLa cells) were fractionated by sucrose density gradient centrifugation, and RNA was detected by absorbance (Abs) at 254 nm. (bottom panels) Fractions were immunoblotted using antibodies indicated at right. Ribosomal proteins L10 and S6 are markers of the 60S and 40S subunits, respectively. The input comes from 5% of the unfractionated ribosomes. Note that bystin was detected in fractions with ribosomal 40S subunits, but not those containing polysomes.

Figure 5 Effect of bystin knockdown by RNAi

Downregulation of bystin inhibits 18S rRNA processing. (A) Effect of siRNA duplexes (50 nM each) identified at the top is shown by immunoblotting for bystin (top) and α-tubulin (bottom). After transfection with siRNAs, cells were incubated in normal medium for 72 h before immunoblotting. Note that siBys-D and siBys-G downregulate bystin protein but control siLuc does not. (B) Pulse-chase analysis of rRNA processing. Cells treated for 72 h with siBys-D (lanes 1-4), siBys-G (lanes 9-12), and control siLuc (lanes 5-8 and 13-16) were labeled with [methyl-^{3}H] methionine and chased for 0-60 min. The resulting fluorogram of the gels is shown.

Note that putative 21S intermediates (indicated by arrow at left) accumulate in siBys-D and siBys-G transfected cells but not in control cells. (C) Pathways of rRNA processing in HeLa cells. The figure is adapted and modified from [33]. Some intermediates larger than 28S are omitted. (D) Cell proliferation assay. Cells were treated with duplexes identified at the bottom and incubated for 96 h, and then cell numbers were counted. Bystin knockdown by siBys-D and siBys-G (black bars) significantly compromised cell viability compared to control siRNA transfected cells (open bar). siTox (hatched bar) was used as an indicator for successful transfection. Values represent means (n = 3); the bars, SD. *$P < 0.05$ (analyzed by *t*-test).

Figure 6 Intracellular localization of bystin under nucleolar stress

(A) HeLa cells were treated with (upper panels) or without (lower panels) ActD and stained with antibodies against bystin (red) and the nucleolar marker fibrillarin (green). Note that bystin disappears from fibrillarin-positive nucleoli after ActD treatment (compare upper (+ ActD) merged image with lower (- ActD)). Bar, 5 μm. (B) HeLa cells treated with ActD (lanes 1-4) and vehicle (lanes 5-8) were subjected to subcellular fractionation as indicated (see Experimental). Each fraction was analyzed by immunoblotting with the antibodies indicated on the right. Note that bystin is not detected in the fractions of nuclei or P100, including cytoplasmic ribosomes, after ActD treatment. See Fig. 2 legend for a definition of markers.

Figure 7 Localization of bystin in HeLa cells under nucleolar and heat stress

(A) HeLa cells transiently overexpressing bystin-FLAG were treated with (upper) and without (lower) ActD and stained with antibodies against bystin (red) and fibrillarin (green). Particles containing bystin in ActD-treated cells are indicated by arrows in merged image (upper panel). (B) Untransfected HeLa cells were incubated at 42^{o}C for 30 min to induce heat shock. Cells were stained with antibodies to detect endogenous

bystin (red) and HSF1 (green). HSF1 is a marker of nuclear stress-induced granules. Nuclear stress-induced granules containing HSF1 are indicated by arrowheads. Note that bystin localization are unchanged under heat shock conditions. (C) HeLa cells transiently overexpressing bystin-FLAG were treated with ActD and stained with antibodies against bystin (red) and HSF1 (green). Note that the particles containing bystin do not colocalize with HSF1. Bars, 5 μm.

Figure 8 Expression of bystin in HeLa and 293T cells before and after treatment with rapamycin

(A) Immunoblotting. HeLa and 293T cells were treated with rapamycin (rap.) and lysed with SDS-PAGE sample buffer. Proteins were separated on 10% SDS-PAGE gels and subjected to immunodetection using antibodies against the proteins indicated on the left. (B) Measurement of expression levels by using immunoblots shown in (A). Band intensities of the proteins in each treatment were determined by using the image analyzer, and the ratio of the intensity of the sample to that of the control was calculated. The ordinates in (B) represent the ratio. Values represent means (n = 3); the bars, SD. The mean of α-tubulin ratios is shown as 1.0. Note that rapamycin partially, but specifically suppressed the expression of bystin, fibrillarin, and ribosomal protein S6 (asterisks, $P < 0.05$).

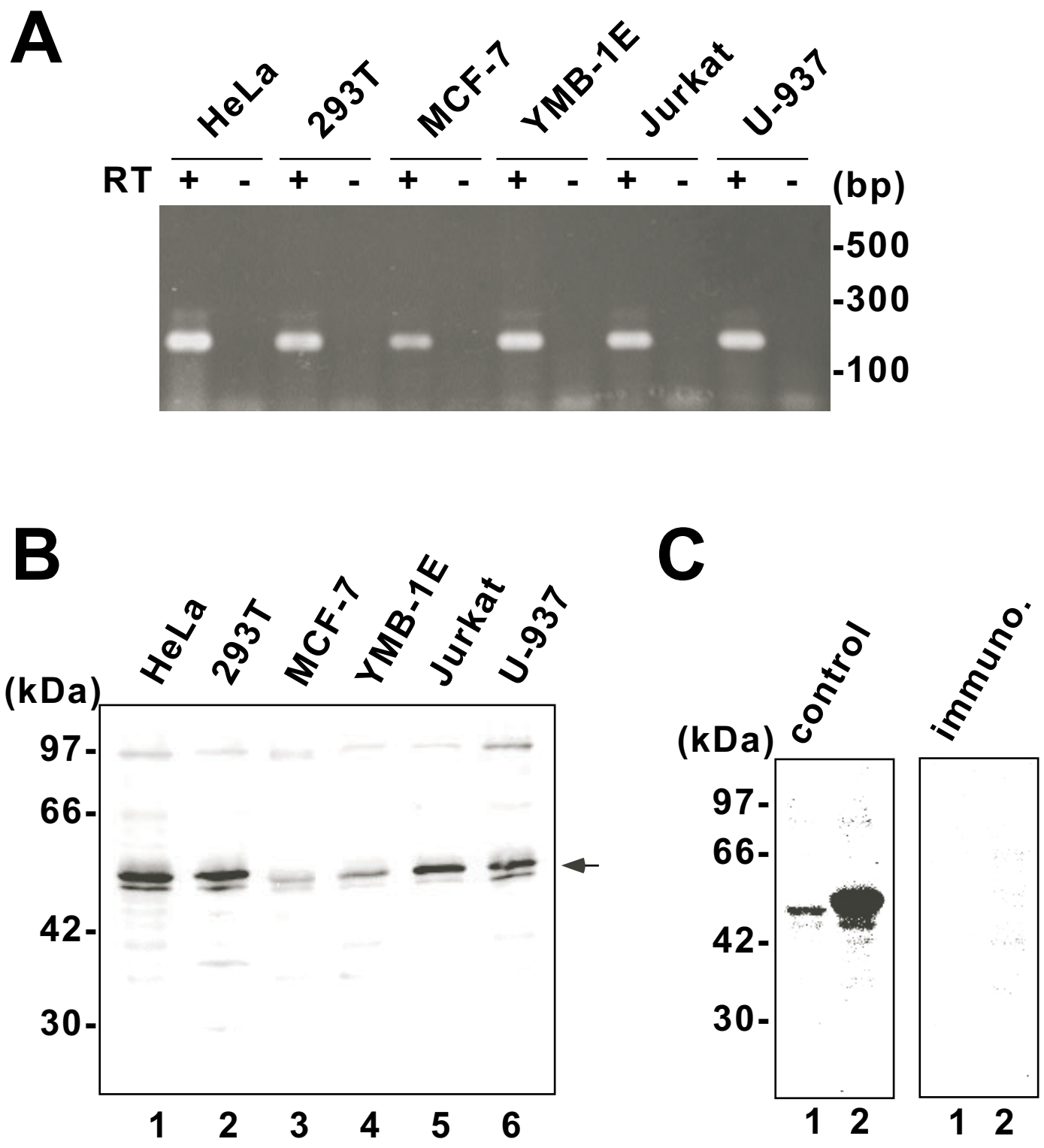

Figure 1 by Miyoshi *et al*.

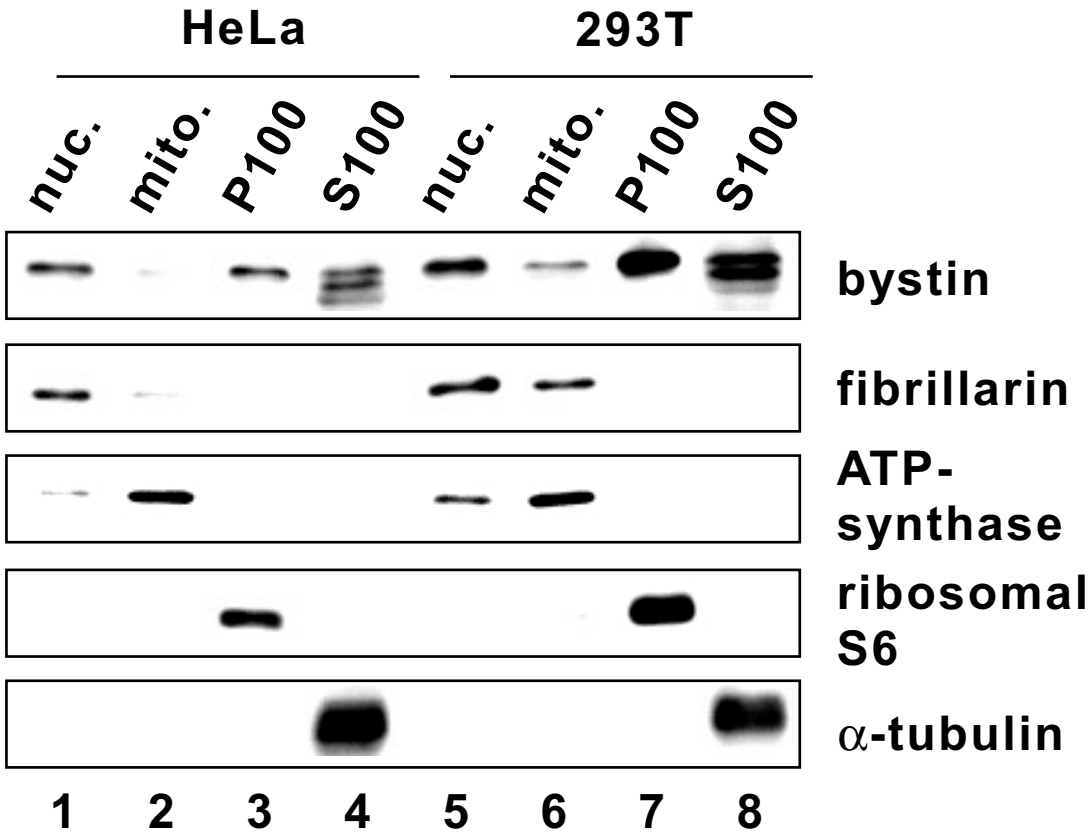

Figure 2 by Miyoshi *et al*.

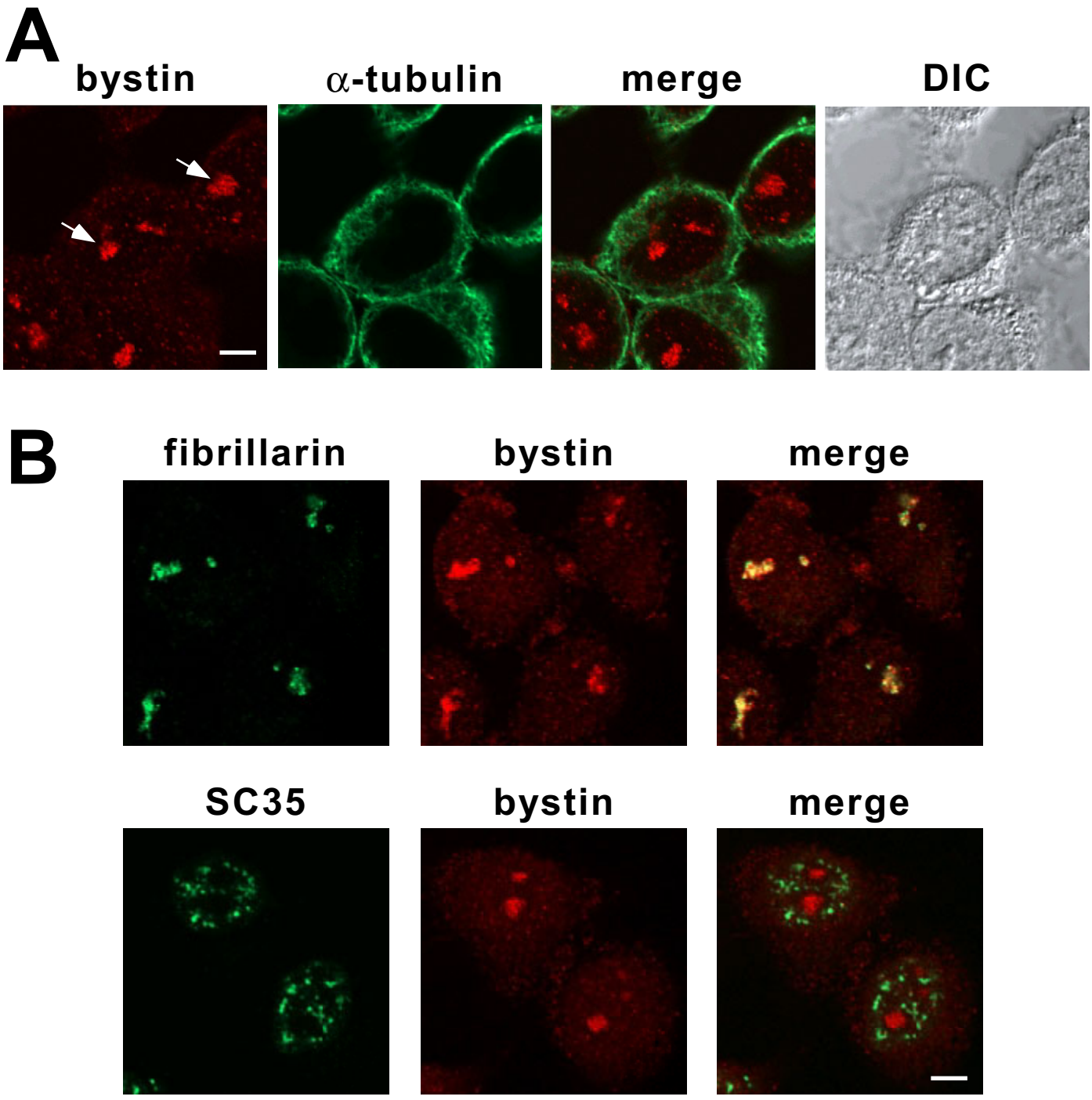

Figure 3 by Miyoshi *et al*.

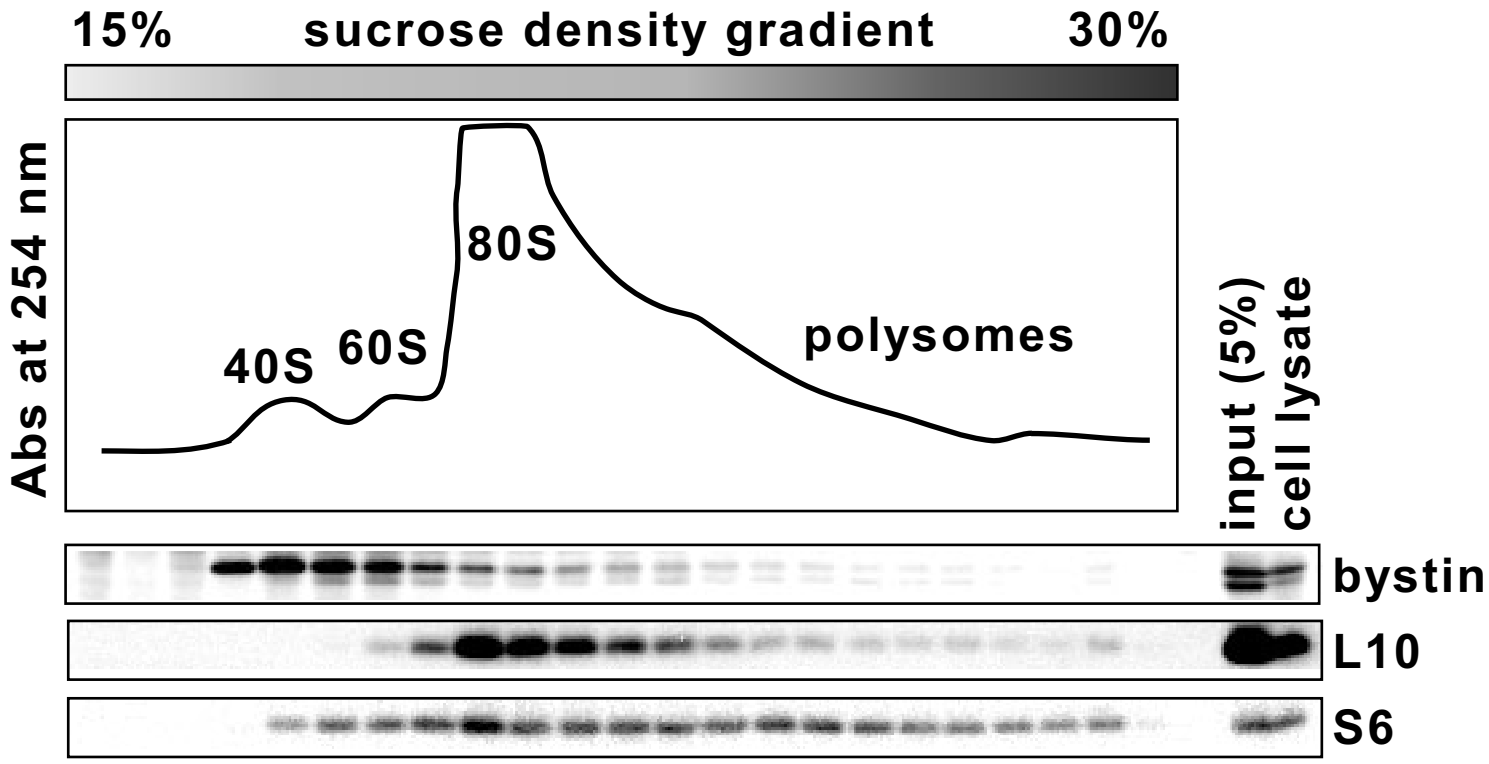

Figure 4 by Miyoshi *et al*.

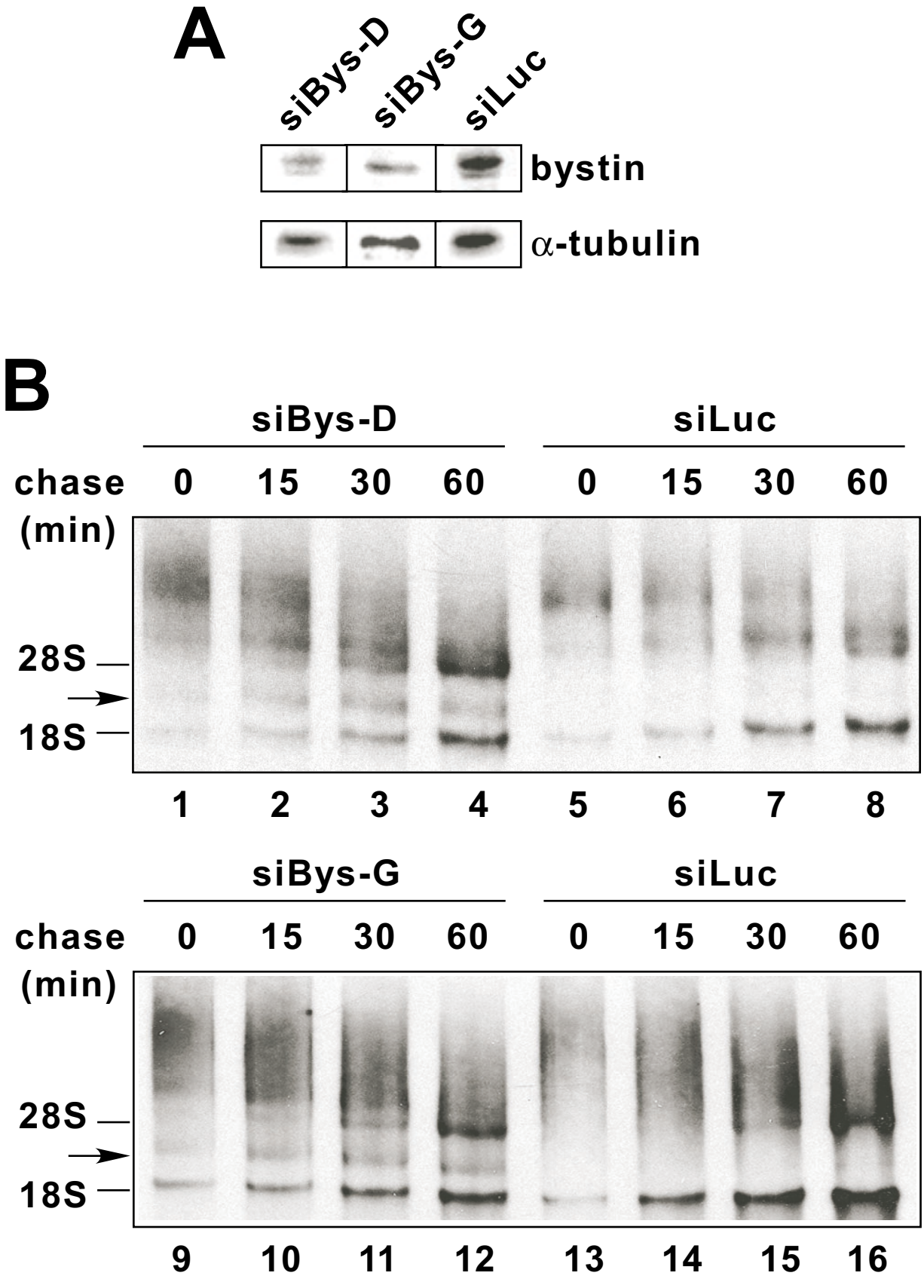

Figure 5 (panels A and B) by Miyoshi *et al*.

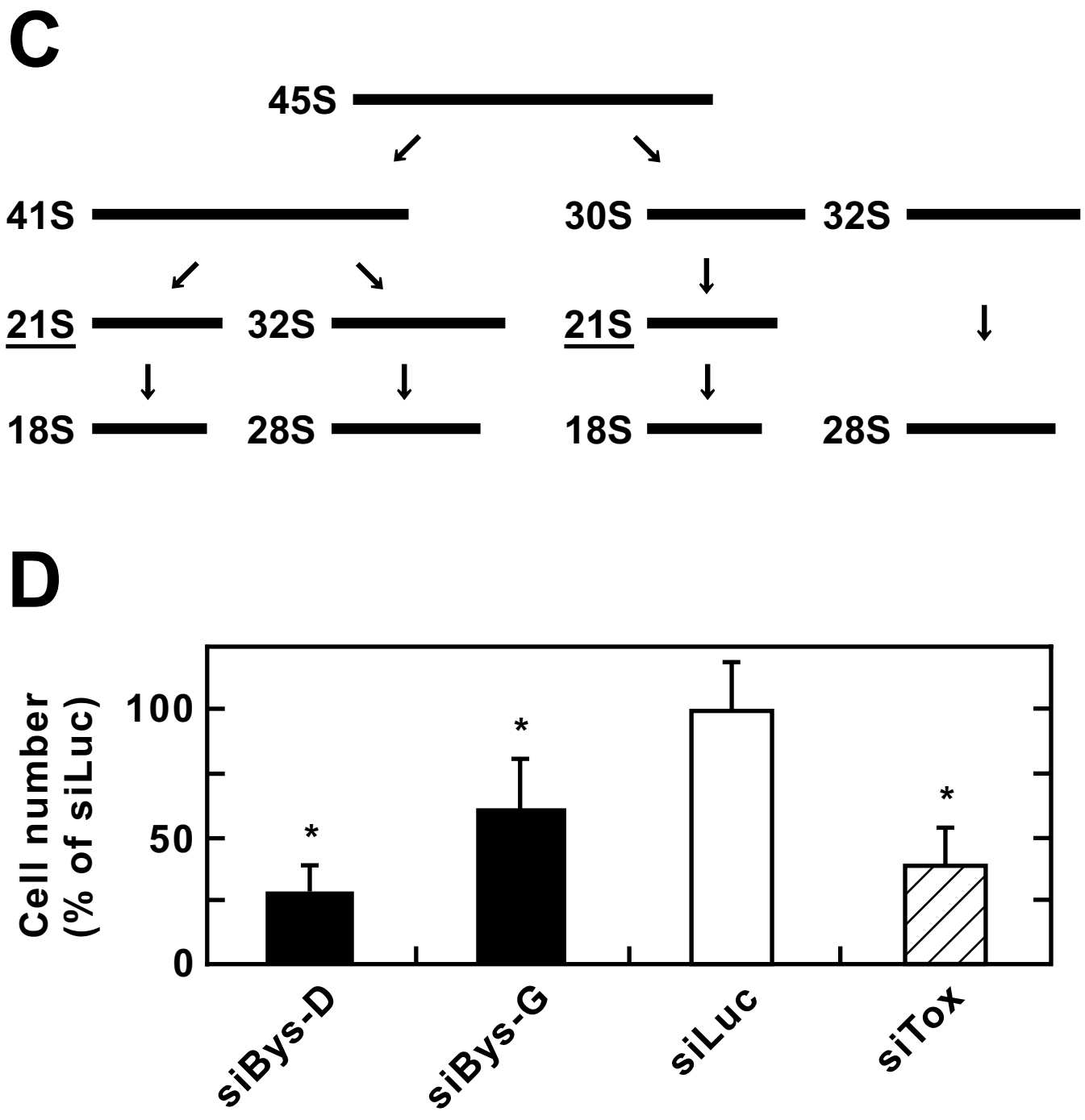

Figure 5 (panels C and D) by Miyoshi *et al*.

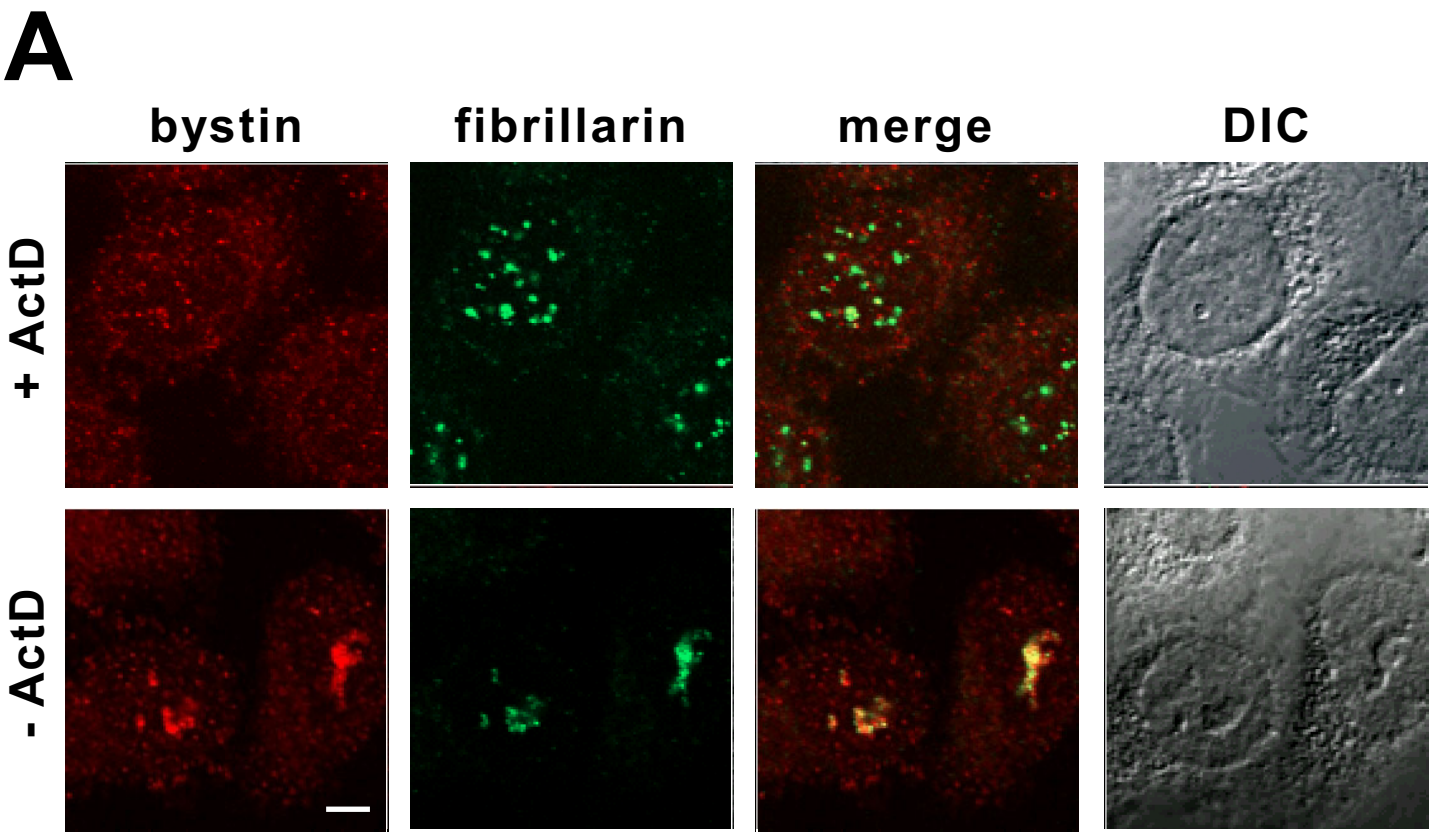

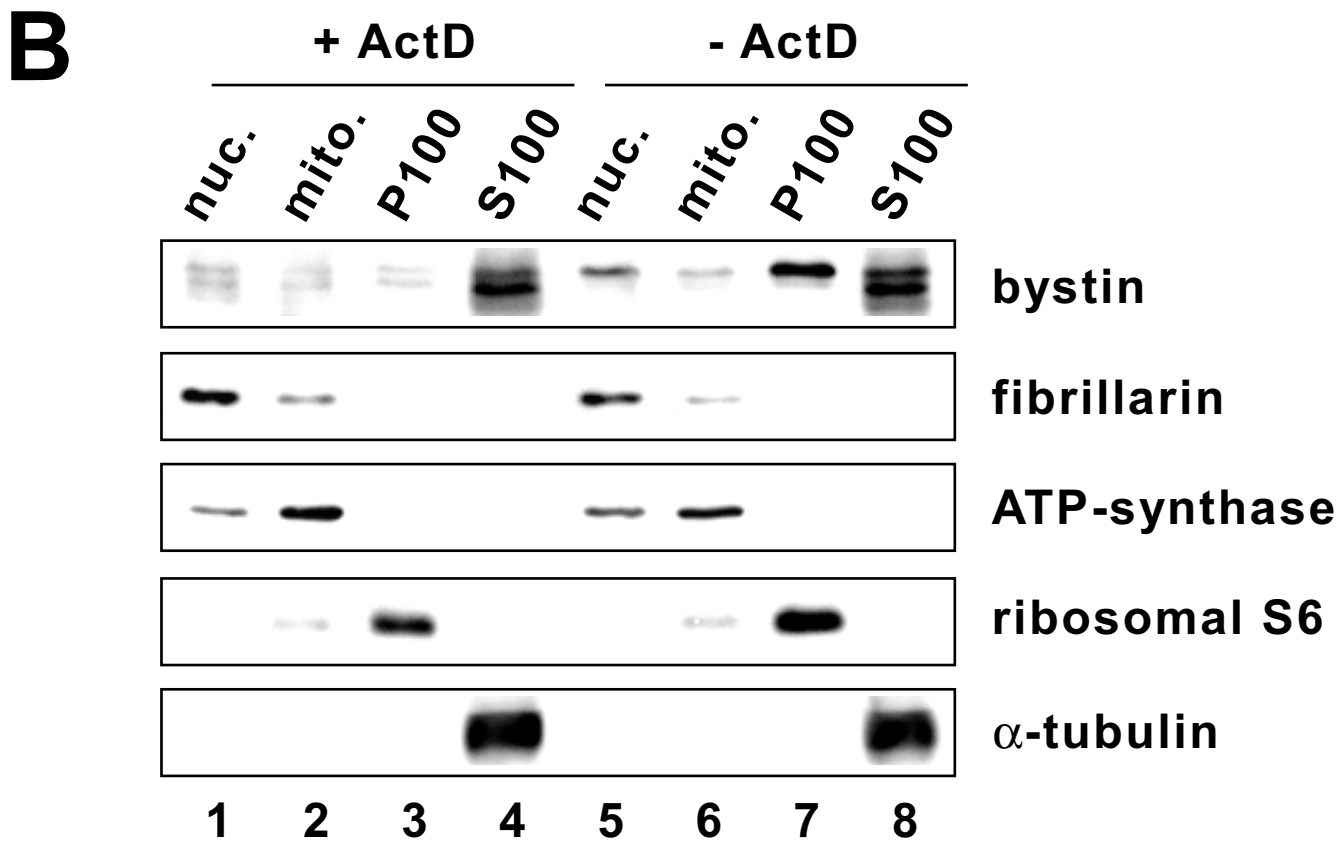

Figure 6 by Miyoshi *et al*.

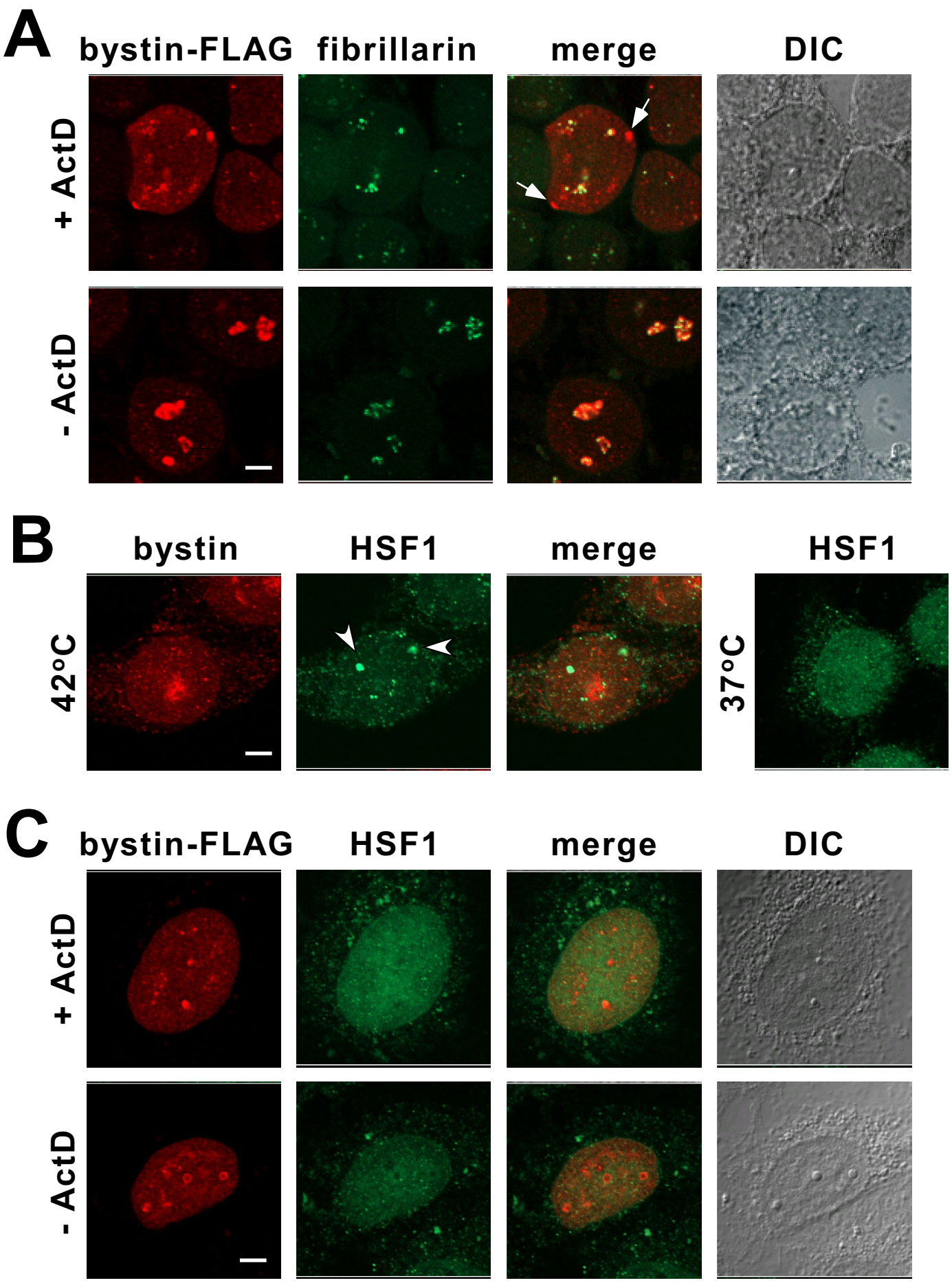

Figure 7 by Miyoshi *et al*.

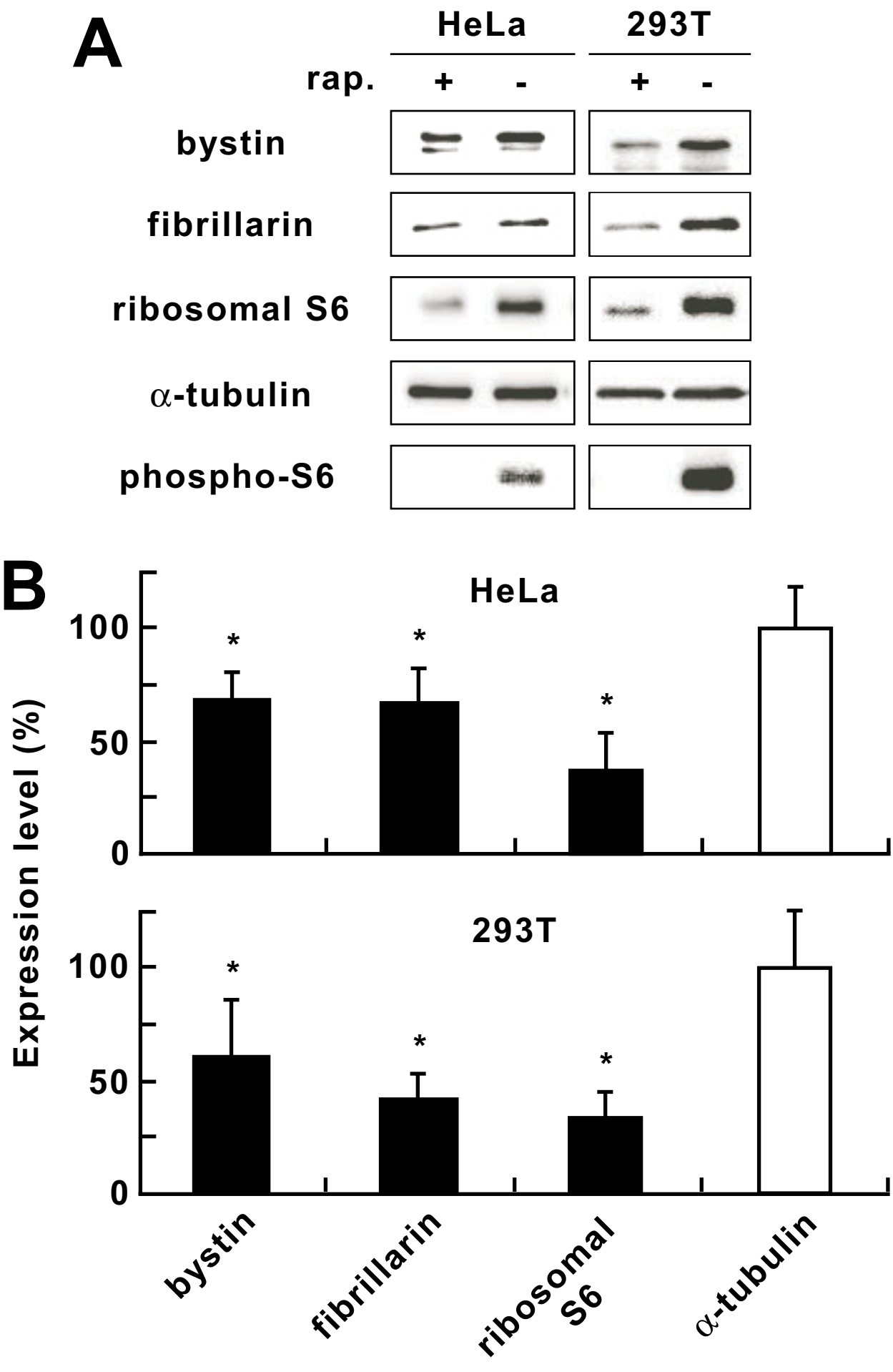

Figure 8 by Miyoshi *et al*.